INTERACTION OF CHOLESTEROL WITH GALACTOCEREBROSIDE AND GALACTOCEREBROSIDE-PHOSPHATIDYLCHOLINE BILAYER MEMBRANES

MARTIN J. RUOCCO AND G. GRAHAM SHIPLEY
Biophysics Institute, Departments of Medicine and Biochemistry, Boston University School of Medicine, Boston, Massachusetts 02118

ABSTRACT The interaction of the galactocerebroside, *N*-palmitoylgalactosylsphingosine (NPGS), with cholesterol has been studied by differential scanning calorimetry (DSC) and x-ray diffraction. Thermal and structural studies demonstrate complex behavior characterized by two endothermic transitions: transition I ($T_I \cong$ 50–60°C) corresponding to an NPGS-cholesterol bilayer gel → bilayer liquid crystal transition and transition II (T_{II} where $T_I < T_{II} < T_{NPGS}$) corresponding to an NPGS bilayer crystal (stable E form) → bilayer liquid crystal transition. For mixtures containing from 6 to 80 mol % cholesterol, x-ray diffraction studies at 22°C ($T < T_I$) indicate two separate lamellar phases; an NPGS crystal bilayer phase and a cholesterol monohydrate phase. For cholesterol concentrations < 50 mol % at $T_I < T < T_{II}$, NPGS-cholesterol liquid crystal bilayer and excess NPGS crystal bilayer phases are observed. For >50 mol % cholesterol concentrations at these temperatures, an excess cholesterol monohydrate phase coexists with the NPGS-cholesterol liquid crystal bilayers. At $T > T_{II}$, complete NPGS-cholesterol miscibility is only observed for <50 mol % cholesterol concentrations, whereas at >50 mol % cholesterol an excess cholesterol phase is present. The solid phase immiscibility of cerebroside and cholesterol at low temperatures is suggested to result from preferential NPGS-NPGS associations via hydrogen bonding. The unique thermal and structural behavior of NPGS-cholesterol dispersions is contrasted with the behavior of cholesterol-phosphatidycholine and cholesterol-sphingomyelin bilayers. Thermal and structural studies of NPGS in dipalmitoylphosphatidylcholine (DPPC)/cholesterol (1:1, molar ratio) bilayers have been performed. For dispersions containing <20 mol % NPGS at 22°C there are no observable calorimetric transitions and x-ray diffraction studies indicate complete lipid miscibility. At >20 mol % NPGS, a high temperature transition is observed that is shown by x-ray diffraction studies to be due to an excess NPGS crystal bilayer → liquid crystal bilayer transition. Complete miscibility of NPGS in DPPC/cholesterol bilayers is observed at $T > T_{NPGS}$. The properties of NPGS/DPPC/cholesterol bilayers are discussed in terms of the lipid composition of the myelin sheath.

INTRODUCTION

The major lipid components of myelin are cholesterol, phospholipid, and galactocerebroside (a glycosphingolipid), which occur in molar ratios ranging from 4:3:2 to 4:4:2 (1). The myelin membrane is compositionally different from other cellular membranes in that it contains a greater percentage of lipid (>70% by weight) than protein (1). This predominantly lipid-containing membrane forms a concentric multilamellar structure that imparts an insulating property to the myelin sheath. Another significant feature of myelin is its unusually large proportion of galactocerebroside (~20 mol %). It is possible that the properties of cerebrosides play a role in regulating the structure and properties of myelin.

The phase behavior and structural properties of galacto- and glucocerebrosides have been well studied (2–10). In particular, hydrated bilayers of synthetic *N*-palmitoylgalactosylsphingosine, NPGS, have been characterized by differential scanning calorimetry (DSC) and x-ray diffraction and shown to exhibit complex stable-metastable polymorphic phase behavior (9). Under appropriate conditions hydrated NPGS forms a highly ordered crystal-like bilayer structure (crystal E phase) characterized by a regular hydrocarbon chain packing. The NPGS bilayer undergoes a crystal E → liquid crystal transition at 82°C (ΔH = 17.5 kcal/mol NPGS), which is reversible only under very slow cooling conditions (9). Hydration studies using DSC indicate that both glucocerebroside and galactocerebroside incorporate only small amounts of tightly bound interbi-

Dr. Ruocco's present address is the Francis Bitter National Magnet Laboratory, Massachusetts Institute of Technology, Cambridge, MA 02139.

layer water, four to five water molecules per cerebroside (11–13). Hydration studies of the crystal bilayer and liquid crystal bilayer phases indicate a low water content of C_{16}-galactocerebroside, which may be related in part to the tight intermolecular packing between the head group/interface regions of adjacent galactocerebroside molecules (13). This tight packing constraint appears to involve the hydrogen bonding capability of the galactose, amide group, and/or sphingosine base (4, 9).

Although the physical properties of galactocerebroside have been extensively studied, its interactions with the other major polar phospholipid components of myelin have not been as thoroughly characterized. Initial physical studies of galactocerebroside and glucocerebroside-phospholipid interactions using ^2H NMR (14–16), DSC (17–19), and Raman spectroscopy (20) have been reported. More recently, the detailed structural and thermal behavior of NPGS in dipalmitoylphosphatidylcholine (DPPC) bilayers has been presented and the phase diagram described (21). This study indicates NPGS has a limiting solubility, i.e., ~23 mol % galactocerebroside in DPPC gel bilayers and DPPC liquid crystal bilayers at temperatures just above the DPPC gel → liquid crystal transition. As the temperature is further increased, the solubility of NPGS in DPPC-rich liquid crystal bilayers increase until at temperatures $>T_c$ (NPGS), NPGS is completely miscible in DPPC bilayers at all molar ratios. The limited miscibility of NPGS at low temperatures is attributed to the capability of galactocerebroside to associate intermolecularly via hydrogen bonding (21).

Cholesterol, the third major lipid component of myelin, is usually a major lipid constituent of plasma membranes. The majority of physical studies have concentrated upon cholesterol-phospholipid interactions because these two lipids are the major constituents of most biomembranes. Since the initial calorimetric studies of Ladbrooke et al. (22), cholesterol has been known to modify the fluidity of the phospholipid hydrocarbon chains. Classically the role of cholesterol in the phospholipid bilayer gel → liquid crystal transition is to diminish the apparent enthalpy change by increasing the gel-state hydrocarbon chain packing disorder while increasing the chain packing order in the liquid crystal state. More recently, numerous studies have addressed the question of the stoichiometry of cholesterol-phospholipid complexes and the maximum solubility of cholesterol in phospholipid bilayers (23–27).

In contrast, there have been few systematic x-ray diffraction and calorimetric studies of cholesterol-glycosphingolipid interactions. Here we address the molecular interaction of cholesterol with C_{16}-galactocerebroside using DSC and x-ray diffraction techniques. Second, in an attempt to understand better the underlying physical properties and behavior of the three major lipid components of myelin, a model membrane system that incorporates cholesterol/phosphatidylcholine (DPPC)/galactocerebroside in molar ratios (1:1:X_{NPGS}), including ratios representative of the myelin membrane lipid composition, has been characterized using the same techniques.

MATERIALS AND METHODS

Samples

N-palmitoylgalactosylsphingosine was synthesized from pig brain cerebroside according to methods described by Skarjune and Oldfield (15). It is estimated that NPGS contains ~5% of the dihydrosphingosine derivative. The purity was checked by thin-layer chromatography (TLC). The NPGS gave a single spot in the solvent system, chloroform/methanol/water/acetic acid (65:25:4:1, vol/vol) and was used without further purification. Certain batches of NPGS containing fatty acid, sphingosine, and other impurities were purified by silicic acid column chromatography, and the final lipid product was recrystallized from chloroform/methanol. The purified lipid gave a single spot by TLC.

Commercial grade DPPC (Calbiochem-Behring Corp., American Hoechst Corp., San Diego, CA) was purified by silicic acid chromatography and shown to be >99% pure by TLC using chloroform/methanol/water/acetic acid (65:25:4:1, vol/vol) as eluting solvent. Commercial grade cholesterol (Nu-Chek Prep., Inc., Elysian, MN) was shown to be >99% pure by TLC using hexane/diethylether/acetic acid (70:30:1, vol/vol).

Sample Preparation

Anhydrous samples of NPGS and cholesterol were weighed to the desired molar ratio directly into a glass tube with a central constriction. The NPGS-cholesterol mixtures were completely dissolved in chloroform methanol (2:1, vol/vol), the solvent evaporated under nitrogen at 30–35°C and the sample placed in a vacuum overnight. Tubes containing various NPGS-cholesterol molar ratios were hydrated (70% H_2O by weight) with the appropriate amount of double-distilled water introduced through a microsyringe. Tubes were purged with nitrogen and immediately flame sealed. Equilibration of the hydrated lipid mixtures was achieved by repeated centrifugation through the constriction for 1–10 min at $T > T_m$ (NPGS), i.e., 82–90°C, followed by longer equilibration periods (1–2 h), at 50–60°C. Ternary lipid mixtures of cholesterol/DPPC/NPGS in 1:1:X_{NPGS} molar ratios were similarly prepared and equilibrated at $T > T_m$ (NPGS) for short periods (1–20 min) followed by longer equilibration periods (1–2 h) at 50–60°C. Equilibrated samples were monitored by TLC and used when determined to have insignificant amounts of impurities. In some instances, lipid mixtures prepared directly into DSC pans were equilibrated by centrifuging the DSC pans at appropriate temperatures. Consistent and reproducible behavior was obtained with both methods of equilibration. Upon equilibration of the sample, the constricted tube was cooled to room temperature, opened, immediately mixed, and well-mixed samples were taken for DSC and x-ray diffraction.

Differential Scanning Calorimetry

Samples taken for calorimetry (1–15 mg) were hermetically sealed in stainless steel pans. Heating and cooling scans over the temperature range 20 to 90°C were performed on a Perkin-Elmer Corp., Instrument Div. (Norwalk, CT) DSC-2 scanning calorimeter using heating/cooling rates of 1.25 to 5°C/min. Isothermal modes were also used. Transition temperatures were determined from the onset of the transition extrapolated to the baseline. Enthalpy measurements were determined from the area under the transition peak by comparison with those for a known standard (gallium). Baselines in the region of the transition were approximated by extrapolating the pretransition baseline to the posttransition baseline. Following the initial equilibration procedure (see Sample Preparation section), samples were heated to $T > T_m$ and cooled to room temperature, incubated at 20–25°C for prolonged periods (12–24 h) before examination by DSC.

X-ray Diffraction

Hydrated samples were transferred to 1-mm (inner diameter) capillaries (Charles Supper Co., Natick, MA). The capillary tubes were flame sealed and placed in a sample holder kept at constant temperature (±0.5°C) by a circulating solvent water bath. Nickel-filtered CuK_α x-radiation (λ = 1.5418 Å) from an Elliot GX-6 rotating anode x-ray generator (Elliot Automation, Borehamwood, England) was focused by either a toroidal mirror optical camera or a double-mirror optical camera. Diffraction patterns were recorded on Kodak No-Screen x-ray film (Eastman Kodak Co., Rochester, NY). Microdensitometry of x-ray photographs was carried out on a microdensitometer (model III-CS; Joyce, Loebl and Co., Ltd., Gateshead-on-Tyne, England).

X-ray diffraction data were also recorded using a position-sensitive detector-counter method. Nickel-filtered CuK_α x-radiation from a microfocus x-ray generator (Jarrel-Ash Div., Fisher Scientific Co., Waltham, MA) was line focused by a single mirror and collimated using the slit optical system of a Luzzati-Baro camera (E^{TS}, Beaudouin, Paris, France). X-ray diffraction data were recorded using a linear position-sensitive detector (Tennelec, Inc., Oak Ridge, TN) and associated electronics (Tracor Northern, Middletown, WI).

RESULTS

NPGS-Cholesterol Bilayers

Differential Scanning Calorimetry. Representative DSC heating thermograms of NPGS/cholesterol binary mixtures in 70% H_2O by weight are presented in Fig. 1. Sample mixtures were prepared as described in the Methods section, cooled to ambient temperatures, incubated at 20°C for prolonged periods (12–24 h), and heated over the 20–90°C temperature range at a rate of 1.25°C/min.

The hydrated stable form of cerebroside (crystal E), exhibits the characteristic high temperature crystal → liquid crystal transition, transition II (Fig. 1 *a*) at 82°C (ΔH = 17.5 kcal/mol NPGS). Addition of small amounts of cholesterol (6.1 and 14.3 mol %. Fig. 1 *b*, *c*, respectively) to NPGS bilayers results in a progressive broadening of the crystal → liquid crystal transition II, and a shift to lower temperatures of the leading edge of this transition. Note the asymmetrical nature of the transition, which gradually rises from the pretransition baseline to the transition peak, beyond which the transition rapidly returns to baseline (Fig. 1 *b*, *c*). At 14.3 mol % cholesterol (Fig. 1 *c*), a broad, low-temperature transition can be detected (transition I), in addition to the cerebroside crystal → liquid crystal transition (transition II). Transition I is centered at 48°C, with a transition enthalpy ΔH = 1.5 kcal/mol NPGS (Fig. 1 *c*). Further addition of cholesterol to NPGS dispersions results in an increase in enthalpy of transition I (Fig. 1 *d–g*). The peak transition temperature also increases from 48 to 56°C.

In contrast to transition I, the NPGS crystal → liquid crystal transition (transition II) diminishes in enthalpy and in transition temperature as >14 mol % cholesterol is added (Fig. 1 *d–f*). At ~50 mol % cholesterol, transition II has decreased in transition temperature to a value (~65°C) slightly above that of transition I and relatively little enthalpy for this transition is exhibited (Fig. 1 *f*). Finally, at cholesterol concentrations >50 mol % cholesterol (e.g., 68.1 mol % cholesterol, Fig. 1 *g*), only the single, low temperature transition I, centered at 56°C, is evident. This relatively cooperative transition is to be contrasted with the well-documented thermal behavior of phospholipid/cholesterol or sphingomyelin/cholesterol mixtures containing >50 mol % cholesterol (22, 28, 30–32), in which only extremely broad, low enthalpy transitions are observed.

Curve decomposition was used to determine the transition enthalpy for T_I and T_{II}. The enthalpies determined from the two transitions are shown in Fig. 2. The cerebroside crystal → liquid crystal transition (T_{II}) decreases from

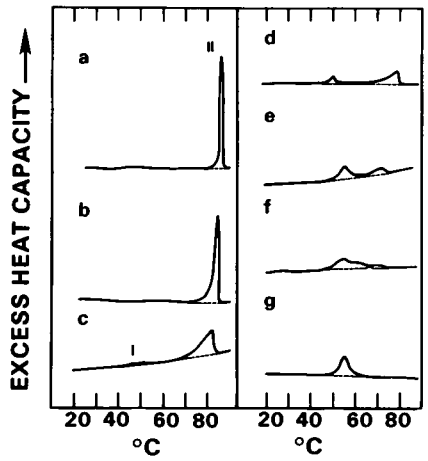

FIGURE 1 DSC thermograms of NPGS/cholesterol mixtures in 70% H_2O by weight. Dispersions were equilibrated at 90°C (see Results section), cooled to 20°C, stored for 12–24 h, and then heated over the 20 to 90°C temperature range. The heating rate equals 1.25°K/min. (*a*) 0, (*b*) 6.1, (*c*) 14.3, (*d*) 28.7, (*e*) 42.9, (*f*) 49.7, (*g*) 68.1 mol % cholesterol. Transitions I and II are indicated, see Results section.

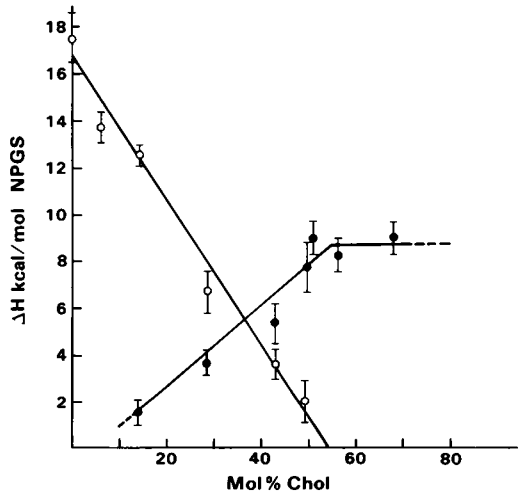

FIGURE 2 Transition enthalpy, ΔH, (kcal/mol NPGS) vs. mol % cholesterol; ●, ΔH of transition I; ○, ΔH of transition II.

17.5 kcal/mol NPGS (0 mol % cholesterol) to 2.0 kcal/mol NPGS at 49.7 mol % cholesterol (open circles in Fig. 2); a least-squares fit yields zero enthalpy at 54 ± 3 mol % cholesterol. The enthalpy of the low temperature transition (T_I) shows a progressive increase from 1.5 kcal/mol NPGS at 14.3 mol % cholesterol to 9.0 kcal/mol NPGS at 49.7 mol % cholesterol (closed circles in Fig. 2). At cholesterol concentrations >50 mol %, there is no significant change in the enthalpy of T_I. The average transition enthalpy of T_I at cholesterol concentrations >50 mol % is 8.7 kcal/mol NPGS.

X-ray Diffraction. X-ray diffraction experiments were performed on cerebroside-cholesterol mixtures that exhibited both transitions I and II and mixtures that exhibited only the low temperature transition I. The structural characteristics of NPGS-cholesterol dispersions at temperatures below transition I (22°C), above transition I (66°C), and above transition II (90°C) were defined.

The x-ray diffraction data for a sample containing a low cholesterol concentration (16.3 mol %) are shown in Fig. 3. The calorimetric thermogram showing the temperatures at which transitions I and II occur and temperatures at which x-ray diffraction experiments were performed (Fig. 3, lettered arrows) is presented with the x-ray diffraction data. At 22°C (arrow A), a temperature below transition I, the NPGS-cholesterol dispersion exhibits an x-ray diffraction pattern (Fig. 3 *A*) that indexes as a lamellar geometry, d = 54 Å. This diffraction pattern is dominated by the diffraction pattern obtained for pure hydrated NPGS bilayers (stable crystal E form, d = 54 Å) shown in Fig. 3 *B* for comparison. In addition to the reflections from the cerebroside phase, reflections at 1/34, 1/17, and 1/5.8 $Å^{-1}$ are also observed (Fig. 3 *A*, upper and lower panels). As shown in the x-ray diffraction pattern (Fig. 3 *A*, lower), these reflections clearly indicate the presence of an excess cholesterol monohydrate crystal phase (for comparison see the x-ray diffraction pattern of cholesterol monohydrate shown in Fig. 3 *D*). The cholesterol monohydrate x-ray diffraction pattern is characterized by two low-angle reflections corresponding to the 001 (1/34 $Å^{-1}$) and 002 (1/17 $Å^{-1}$) reflections (low-angle region of diffraction pattern *D* in Fig. 3). Wide-angle reflections also occur at 1/5.8, 1/4.7, and 1/3.7 $Å^{-1}$ (arrows in wide-angle region of diffraction pattern Fig. 3 *D*). This diffraction pattern exhibits absences of strong hkl reflections in the 1/6 → 1/10 $Å^{-1}$ region and the presence of a strong 1/5.8 $Å^{-1}$ reflection, both distinctive features of a cholesterol monohydrate crystal phase (27). Because reflections characteristic of NPGS and cholesterol monohydrate crystals are

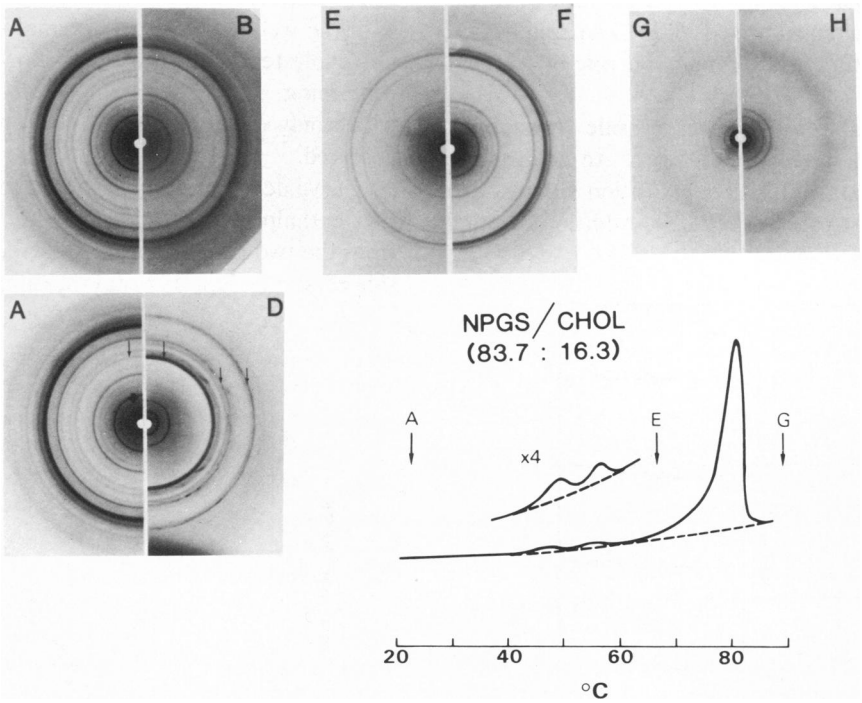

FIGURE 3 DSC and x-ray diffraction data of a NPGS/cholesterol (83.7:16.3, mol %) bilayers. Samples were equilibrated as described in Results section. DSC thermogram is a representative heating scan; lettered arrows indicate temperatures at which x-ray diffraction experiments were performed and correspond to the lettered x-ray diffraction patterns shown. X-ray diffraction data: *A* (*upper* panel) NPGS/cholesterol (83.7:16.3) bilayers at 22°C; *A*, (*lower* panel), same as *A*, *upper* panel, arrow indicates 1/5.8 $Å^{-1}$ reflection of cholesterol monohydrate phase; (*B*) hydrated NPGS (stable E form, see Results and reference 9) at 22°C; (*D*) cholesterol monohydrate at 22°C, arrows indicate strong wide-angle reflections at 1/5.8, 1.47, and 1/3.7 $Å^{-1}$; (*E*) NPGS/cholesterol bilayers at 66°C; (*F*) hydrated NPGS (stable E form) at 66°C; (*G*) NPGS/cholesterol bilayers at 90°C; (*H*) hydrated NPGS at 90°C.

apparent in the diffraction pattern shown in Fig. 3 *A* (upper and lower panels), both crystal phases coexist separately at 22°C.

Heating above the complex, low temperature transition I to 66°C (arrow E) gives the x-ray diffraction pattern shown in Fig. 3 *E*. In this diffraction pattern there is no evidence of the cholesterol monohydrate reflections. The diffraction pattern is dominated by reflections from the NPGS crystal bilayers (stable form E); compare with the x-ray diffraction pattern of NPGS bilayers (stable form E) at 66°C (Fig. 3 *F*). What are not clearly observed at this low cholesterol concentration are reflections associated with NPGS–cholesterol-containing bilayers. Although this phase becomes more apparent at higher cholesterol contents (see below), the difficulty in defining this phase is illustrated in Fig. 4. The diffraction pattern of a NPGS dispersion containing 29 mol % cholesterol at 22°C (Fig. 4 *b*) shows reflections (small arrows) from an excess cholesterol monohydrate phase. The second-order reflection at 1/27 $Å^{-1}$ of the NPGS crystal phase is also indicated (large arrow). For comparison, the x-ray diffraction pattern of pure NPGS bilayers at 22°C is shown in Fig. 4 *a*. At 66°C, the reflections associated with the cholesterol monohydrate phase disappear (Fig. 4 *c*). Evidence that cholesterol is incorporated into disordered NPGS bilayers is not clear because the periodicity of the NPGS-cholesterol liquid crystal bilayers is similar to that of the crystal NPGS bilayers. Supporting evidence for this is provided by the x-ray diffraction pattern shown in Fig. 4 *d*. At 66°C an NPGS dispersion containing 50 mol % cholesterol in which all NPGS has been melted yields a single liquid crystal phase with a lamellar periodicity of 54 Å and a broad, diffuse wide-angle reflection at 1/4.8 $Å^{-1}$. Note that although the x-ray diffraction pattern in Fig. 4 *c* is dominated by reflections from the NPGS crystal phase, particularly in the wide-angle region, a broad underlying reflection at ~1/5 $Å^{-1}$ is observed (small arrows, Fig. 4 *c*), which is not present at 22°C (Fig. 4 *b*), in pure NPGS bilayers at 22°C (Fig. 4 *a*), or pure NPGS bilayers at 66°C (Fig. 3 *F*). Thus, it can be concluded that the x-ray diffraction pattern at 66°C shown in Fig. 3 *E* is representative of two lipid phases: an NPGS crystal (stable form E) phase and an NPGS-cholesterol liquid crystal phase.[1]

Returning to Fig. 3, further heating of the 16.3 mol % cholesterol containing dispersion beyond transition II to 90°C (arrow G) melts the remaining NPGS crystal bilayers to give a diffraction pattern exhibiting a single set of lamellar reflections indexing on a 53-Å periodicity and a

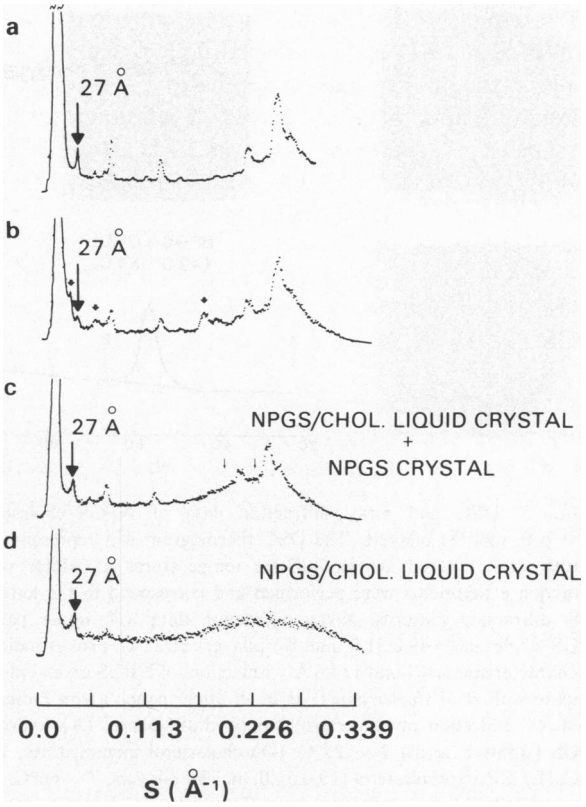

FIGURE 4 X-ray diffraction patterns of NPGS/cholesterol bilayers. (*a*) hydrated NPGS (stable E form) T = 22°C, large arrow indicates second-order lamellar reflection of NPGS bilayer phase; (*b*) NPGS/cholesterol (71:29, mol %) bilayers, T = 22°C; large arrow indicates second-order lamellar reflection of NPGS (stable form), small arrows indicate the 001, 002, and 1/5.8 $Å^{-1}$ reflections of cholesterol monohydrate phase, see Results; (*c*) same as in *b*, T = 66°C; (*d*) NPGS/cholesterol (50:50, mol %) bilayers, T = 66°C. A Luzzati-Baro camera geometry with a position-sensitive detector was used to collect the data.

diffuse 1/4.8-$Å^{-1}$ reflection (Fig. 3 *G*). This corresponds to a single NPGS-cholesterol liquid crystal phase in which the intensity distribution and positions of the low-angle reflections differ from those of pure NPGS liquid crystal bilayers at 90°C (compare Fig. 3 *H*).

Mixtures at higher cholesterol contents exhibit less complicated structural behavior. Fig. 5 summarizes the x-ray diffraction data for an NPGS-cholesterol dispersion containing 51 mol % cholesterol. At this lipid composition, only a single endotherm (transition I) is observed. At 22°C (arrow A), a temperature below the low temperature transition (I), the diffraction pattern shown in Fig. 5 *A* (upper and lower panels) is recorded. This x-ray diffraction pattern clearly exhibits reflections from both the NPGS crystal and cholesterol monohydrate phases; compare Fig. 5 *A* (upper panel) with the x-ray diffraction pattern of the NPGS bilayers at 22°C (Fig. 5 *B*); arrows in Fig. 5 *A* (upper panel) correspond to wide-angle reflections of the NPGS crystal bilayer phase; also, compare Fig. 5 *A* (lower panel) with the x-ray diffraction pattern of crystal-

[1]Corroborating evidence for the presence of two lipid phases was recently obtained in a solid state ^{2}H-NMR study of [7,7-$^2H_2$]-NPGS/cholesterol bilayer dispersions in the 50–70°C range. ^{2}H-NMR spectra clearly indicate the presence of overlapping gel phase and liquid crystal phase spectral line shapes at these temperatures (Ruocco, M. J., D. J. Siminovitch, S. K. Das Gupta, and R. G. Griffin, manuscript in preparation).

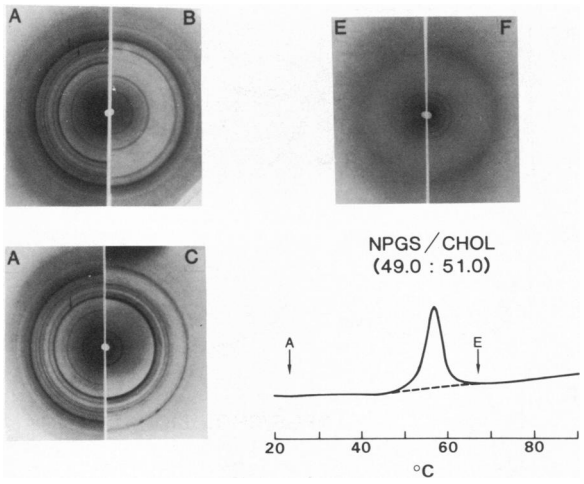

FIGURE 5 DSC and x-ray diffraction data of NPGS/cholesterol (49.0:51.0, mol %) bilayers. The DSC thermogram is a representative heating scan; lettered arrows indicate temperatures at which x-ray diffraction experiments were performed and correspond to the lettered x-ray diffraction patterns. X-ray diffraction data: (*A*, *upper* panel) NPGS/cholesterol (49.0:51.0, mol %) bilayers at 22°C, arrows indicate the characteristic 1/4.1 and 1/4.6 $Å^{-1}$ reflections of NPGS crystal phase, compare with *B*; *A* (*lower* panel) as in *A*, *upper* panel, arrow indicates 1/5.8-$Å^{-1}$ reflection of cholesterol monohydrate phase; (*B*) hydrated NPGS (stable E form) T = 22°C; (*D*) cholesterol monohydrate, T = 22°C; (E) NPGS/cholesterol (49.0:51.0, mol %) bilayers, T = 66°C; (*F*) hydrated NPGS liquid crystal bilayers, T = 90°C, compare with melted NPGS bilayers containing 51 mol % cholesterol in *E*.

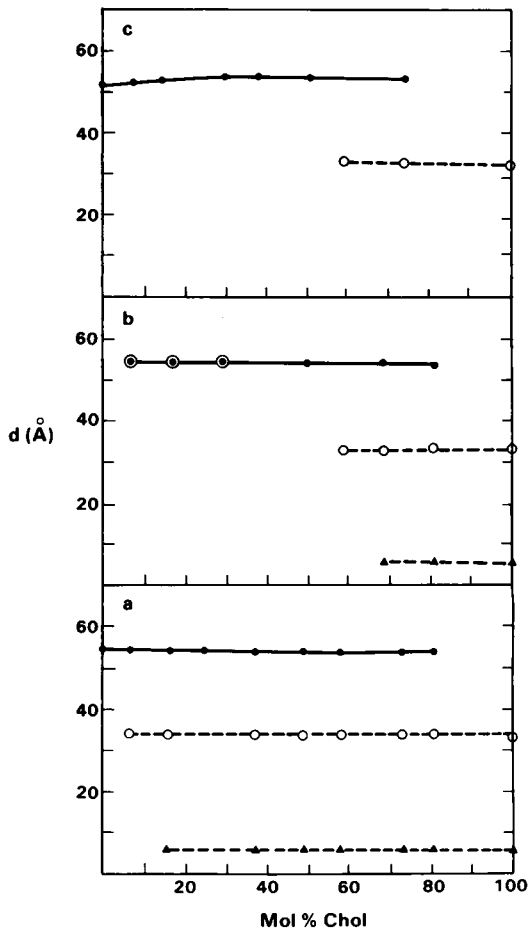

FIGURE 6 Lamellar periodicities, d, vs. mol % cholesterol at (*a*) T = 22°C; ●, NPGS crystal (stable E form) bilayers; ○, cholesterol monohydrate 001 reflection; ▲, 1/5.8 $Å^{-1}$ reflection of cholesterol monohydrate; (*b*) T = 66°C; ⊙, lamellar periodicities of NPGS crystal (stable E form) bilayers and NPGS/cholesterol liquid crystal bilayers at cholesterol concentrations <50 mol %; ●, NPGS/cholesterol liquid crystal bilayers at concentrations >50 mol % cholesterol; ○, 001 reflection and ▲, 1/5.8-$Å^{-1}$ reflection of cholesterol monohydrate phase; (*c*) T = 90°C; ●, NPGS/cholesterol liquid crystal bilayers; ○, 001 reflection of anhydrous cholesterol.

line cholesterol monohydrate at 22°C (Fig. 5 *C*). This behavior is similar to that observed at lower cholesterol concentrations where two separate crystal phases coexist (see Fig. 3 *A* upper and lower panels). At a temperature above the single transition I, 66°C (arrow E), a single set of lamellar reflections of periodicity 54 Å and a diffuse 1/4.8-$Å^{-1}$ reflection are observed (Fig. 5 *E*), indicating a single liquid crystal bilayer phase. The x-ray diffraction pattern of liquid crystal NPGS bilayers at 90°C is shown for comparison (Fig. 5 *F*).

X-ray diffraction studies of NPGS-cholesterol mixtures over a large cholesterol concentration range, 6 to 80.5 mol %, were performed at 22, 66, and 90°C. These results are summarized in Fig. 6. At 22°C, lamellar periodicities characteristic of both the NPGS stable crystal bilayer phase (d = 54 Å; Fig. 6 *a*, solid circles) and the cholesterol monohydrate phase (d = 34 Å; Fig. 6 *a*, open circles) were observed over the 6 to 80.5 mol % cholesterol concentration range. The 1/5.8-$Å^{-1}$ reflection, characteristic of the cholesterol monohydrate phase, is also observed over a similar range (Fig. 6 *a*, triangles). At 66°C, a single periodicity is observed at cholesterol concentrations <50 mol % cholesterol. The similarity of the lamellar periodicities of the NPGS crystal bilayer phase (d = 54 Å) and the NPGS-cholesterol liquid crystal bilayer phase $d \cong 54$ Å) does not allow resolution of the two sets of periodicities. Note that at cholesterol concentrations <50 mol %, there are no reflections characteristic of the cholesterol monohydrate phase at 1/34 or 1/5.8 $Å^{-1}$ (see Figs. 3 *E*, 4 *c* and compare Figs. 6 *a* and *b*). However, at concentrations >50 mol % cholesterol, these reflections are observed (Fig. 6 *b*, open circles and closed triangles) in addition to the lamellar periodicity corresponding to only the NPGS-cholesterol liquid crystal bilayers (Fig. 6 *b*, closed circles). Therefore, at 66°C, mixtures containing >50 mol % cholesterol exhibit two separate phases, an NPGS-cholesterol liquid crystal bilayer phase containing ~50 mol % cholesterol and a separate cholesterol monohydrate phase. At 90°C, above transition II, a single lamellar periodicity is observed at concentrations <50 mol % cholesterol (Fig. 6 *c*, solid circles). This periodicity corresponds to a single lamellar NPGS-cholesterol phase. Note that at 90°C, pure NPGS liquid crystal bilayers give a lamellar periodicity of 51.5 Å. This lamellar periodicity increases slightly to 54 Å with the

addition of cholesterol over the 0–50 mol % cholesterol concentration range. At cholesterol concentrations >50 mol %, a second reflection is observed at 1/34 $Å^{-1}$ due to an excess cholesterol phase. Note that at 90°C, the excess cholesterol phase is in the anhydrous crystal form (27).

NPGS/Cholesterol/Phospholipid Bilayers

Differential Scanning Calorimetry. The reproducible calorimetric behavior of dispersions of cholesterol/DPPC, 1:1 molar ratio, containing various molar percentages of NPGS is summarized in Fig. 7. The cholesterol/DPPC bilayers containing no cerebroside show no detectable cooperative thermal transition (Fig. 7 *a*). This behavior is characteristically found for phosphatidylcholine dispersions containing ~50 mol % cholesterol (22).

When cerebroside is added to the DPPC/cholesterol (1:1) bilayers, no detectable thermal transition is observed (Fig. 7 *b*, *c*) until ~27.3 mol % NPGS (Fig. 7 *d*). The 27.3 mol % NPGS dispersion exhibits a broad endotherm centered at 60.8°C with an enthalpy of 1.8 kcal/mol NPGS. As increasing amounts of cerebroside are added from 27.3 to 55.5 mol % NPGS, the peak transition temperature increases from 60.8 to 73.8°C and the transition enthalpy also increases (Fig. 7 *e*, *f*). The transition temperature and enthalpy data are summarized in Fig. 8 *a*, *b*, respectively.

Dispersions containing <27 mol % NPGS exhibit no observable thermal transitions. In contrast, samples containing 34.8, 40.9, and 55.5 mol % NPGS yield broad endothermic transitions with ΔH = 2.8, 4.7, and 6.1 kcal/mol NPGS, respectively (see Fig. 8 *b*). The enthalpy data in Fig. 8 demonstrate a monotonic increase with mol % NPGS. The enthalpy of the pure hydrated NPGS crystal → liquid crystal transition (ΔH = 17.5 kcal/mol NPGS) is also plotted in Fig. 8. The best least-squares fit of these data indicate an intercept on the abscissa of 22 ± 3 mol % NPGS, where no calorimetric transition should be observed.

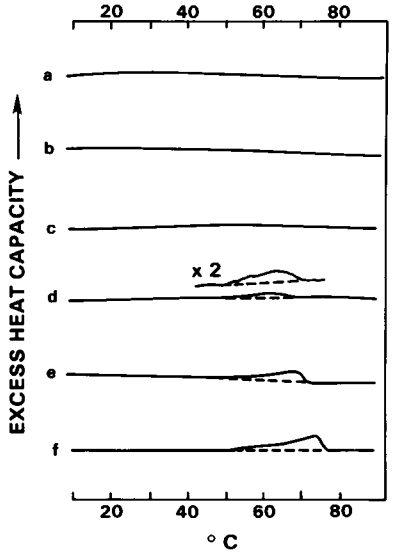

FIGURE 7 DSC thermograms of DPPC/cholesterol (1:1 molar ratio)/NPGS bilayers containing (*a*) 0; (*b*) 9.7; (*c*) 23.1; (*d*) 27.3; (*e*) 40.8; (*f*) 55.5 mol % NPGS. The heating rate equals 1.25°K/min.

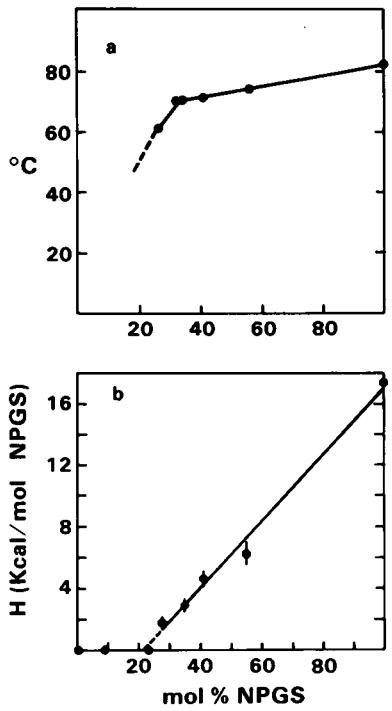

FIGURE 8 (*a*) Transition temperature (T_{peak}) and (*b*) transition enthalpy, ΔH (kcal/mol NPGS), of the endothermic transition in Fig. 7 for DPPC/cholesterol/NPGS bilayers.

X-ray Diffraction. Structural experiments were performed at temperatures below (22°C) and above (90°C) the broad endothermic transition (see Fig. 7). At 22°C, the x-ray diffraction pattern for the DPPC/cholesterol (1:1 molar ratio) dispersion is shown in Fig. 9 *A*. The diffraction pattern shows four lamellar reflections, *d* = 64.7 Å. The wide-angle region is characterized by a broad diffuse reflection at ~1/4.6 $Å^{-1}$ (arrow). This diffraction pattern is characteristic of a cholesterol-containing DPPC bilayer liquid crystal phase. As increasing amounts of NPGS are added to the DPPC/cholesterol dispersion (i.e., from 0 to 17.8 mol %), similar diffraction patterns are recorded in which the single lamellar periodicity decreases slightly from 64.7 to 63.8 Å. For >20 mol % NPGS, no further change in *d* for the DPPC/cholesterol-rich dispersions is observed (Fig. 10). The lamellar periodicity remains constant at 63.8 Å. At cerebroside concentrations greater than ~20 mol % NPGS, a second lamellar phase is observed in addition to the cholesterol/DPPC-rich lamellar phase. An example of this two phase system containing 40.9 mol % NPGS is shown in Fig. 9 *B*. At this cerebroside content, the diffraction pattern is clearly dominated by reflections characteristic of the excess cerebroside crystal

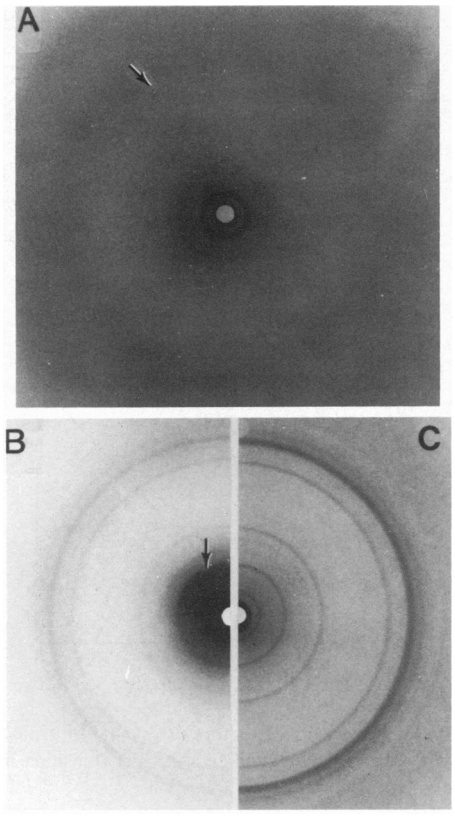

FIGURE 9 X-ray diffraction patterns of (*A*) DPPC/cholesterol (1:1, molar ratio) bilayers, T = 22°C (arrow indicates 1/4.6-Å^{-1} reflection); (*B*)-DPPC/cholesterol (1:1, molar ratio) bilayers containing 40.9 mol % NPGS, T = 22°C, arrow corresponds to fourth-order lamellar reflection of excess NPGS phase; (*C*) hydrated NPGS (stable E form), T = 22°C.

phase (compare Fig. 9 *B* with the diffraction pattern for pure hydrated NPGS at 22°C in Fig. 9 *C*). At all concentrations >20 mol % NPGS, two lamellar periodicities are observed, arising from a cholesterol/DPPC-rich liquid crystal bilayer phase ($d \cong 64$ Å) and an NPGS crystal phase ($d \cong 54$ Å) (see Fig. 10).

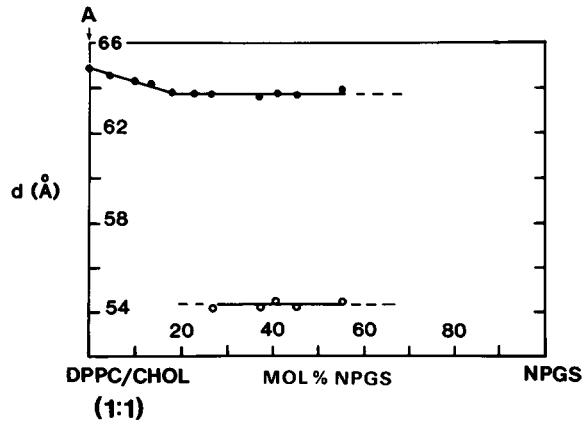

FIGURE 10 Lamellar periodicity, d, of DPPC/cholesterol (1:1 molar ratio)/NPGS dispersions as a function of NPGS concentration at T = 22°C: ●, DPPC/cholesterol-rich bilayer phase; ○, NPGS (stable E form) bilayer phase.

At 90°C, the diffraction pattern from the cholesterol/DPPC (1:1 molar ratio) bilayers containing no cerebroside gives a reduced lamellar periodicity of 61 Å (Fig. 11 *a*), compared with the bilayer periodicity at 22°C (d = 65 Å) (Figs. 9 *A* and 10). The diffraction pattern of DPPC/cholesterol bilayers containing 34.8 mol % NPGS at 90°C is shown in Fig. 11 *b* for comparison. This diffraction pattern also gives a single lamellar periodicity of 57.6 Å; note that the intensity distribution is different compared with the diffraction pattern of pure DPPC/cholesterol bilayers. Mixtures containing various amounts of NPGS gave single lamellar phases, in which the periodicity progressively decreased from 61 Å (0 mol % NPGS) to 51.5 Å (100 mol % NPGS) as shown in Fig. 12. This linear dependence of lamellar periodicity is indicative of lipid miscibility.

DISCUSSION

NPGS-Cholesterol Bilayers

Cerebroside-cholesterol mixtures exhibit complex thermal behavior characterized by two endothermic transitions over the temperature range 20 to 90°C. For <50 mol % cholesterol concentrations, a high temperature NPGS crystal → liquid crystal transition (II) is present. Although this transition is present at these concentrations, the transition enthalpy (Fig. 2) and the temperature at which this transition occurs (Fig. 1) decreases with increasing cholesterol concentration. At ~50 mol % cholesterol, transition II is no longer observed. Over the same cholesterol concentration range (0–50 mol %), a second complex, low temperature transition (I) also occurs (Figs. 1 *b–e* and 3). In contrast to transition II, transition I increases in both transition temperature and enthalpy until 50 mol % cholesterol, beyond which only a single transition I is observed with a constant ΔH = 8.7 kcal/mol NPGS (Fig. 2).

X-ray diffraction studies at 22°C over the entire cholesterol concentration range studied (6 to 80.5 mol % cholesterol) indicate the presence of two phases, a hydrated NPGS stable crystal E form (d = 54.5 Å), and a cholesterol monohydrate crystal form (d = 34 Å). These results indicate that at low temperatures (i.e., 22°C) cerebroside

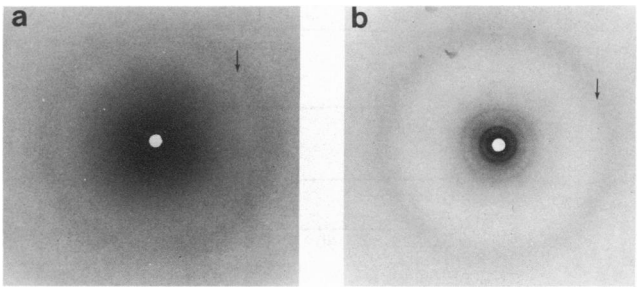

FIGURE 11 X-ray diffraction patterns of DPPC/cholesterol (1:1, molar ratio)/NPGS bilayers containing (*a*) 0; (*b*) 34.8 mol % NPGS. Temperature = 90°C.

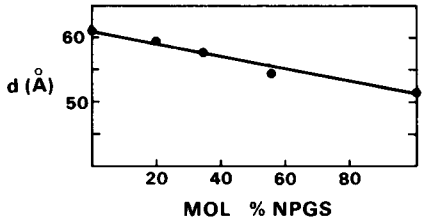

FIGURE 12 Lamellar periodicity, d, of DPPC/cholesterol (1:1 molar ratio)/NPGS bilayers as a function of NPGS concentration. Temperature = 90°C.

and cholesterol exhibit solid phase immiscibility. For NPGS-cholesterol mixtures that exhibit a low temperature transition I, structural studies indicate that at concentrations <50 mol % cholesterol, the cerebroside bilayers melt at reduced temperatures compared with hydrated NPGS bilayers, forming a NPGS liquid crystal bilayer containing cholesterol (Figs. 3 and 4). The bilayer periodicity of this melted liquid crystal bilayer phase is similar to the unmelted NPGS crystal bilayer phase, therefore making difficult the resolution of reflections from coexisting NPGS liquid crystal bilayers containing cholesterol (see, for example, Figs. 3 and 4). For <50 mol % cholesterol, residual crystalline cerebroside (d = 54 Å) remains until at temperatures $>T_M$ (NPGS) the remaining NPGS melts into the preexisting NPGS-cholesterol phase forming a single liquid crystal phase (Figs. 3, 4, and 6). At >50 mol % cholesterol, x-ray diffraction studies at 66°C indicate that NPGS bilayers melt yielding a single NPGS-cholesterol liquid crystal bilayer phase containing 50 mol % cholesterol (Figs. 4–6) and an excess cholesterol monohydrate phase (Fig. 6). At 90°C, a temperature beyond which cholesterol monohydrate loses its single water of hydration (T = 86°C, see reference 27), an anhydrous cholesterol phase coexists with the NPGS-cholesterol-containing bilayers.

The phase diagram is constructed from the calorimetric and x-ray diffraction data and shown in Fig. 13. The phase boundaries are constructed from the $T_{initial}$ and T_{final} of the calorimetric thermograms presented in Fig. 1. The onset and completion temperatures of transition I are plotted as solid and open squares, respectively. The onset and completion temperatures of transition II (for cholesterol concentrations <50 mol %) are plotted as solid and open triangles, respectively. Below the transition I onset temperature, a two phase system, cerebroside bilayer and cholesterol monohydrate crystal, exists over the concentration range 6.1 to 80.5 mol % cholesterol. The structures of the NPGS bilayer and cholesterol crystal phases are shown schematically in Fig. 13. At <50 mol % cholesterol, an NPGS crystal phase coexists with an NPGS-cholesterol liquid

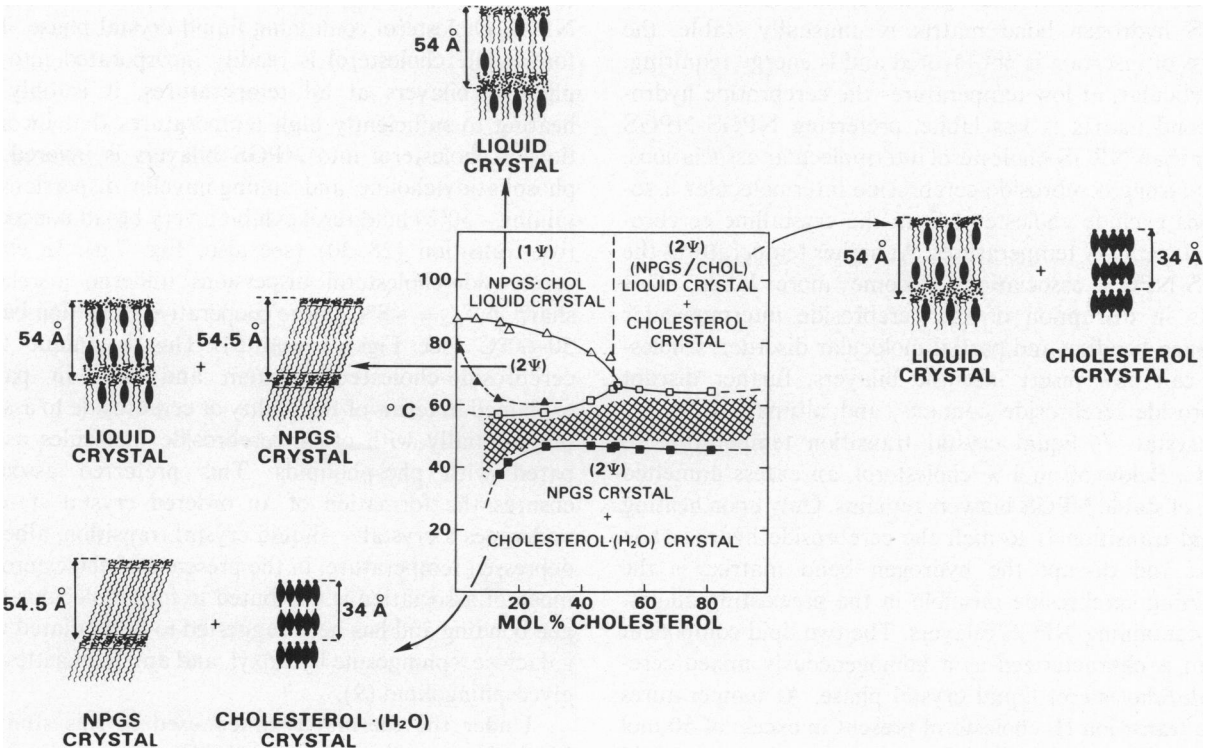

FIGURE 13 Temperature-composition phase diagram of NPGS/cholesterol binary lipid system at 70% H_2O by weight. Onset and completion temperatures for transition I are plotted as ■ and □, respectively. Onset and completion temperatures for transition II are plotted as ▲ and Δ, respectively. The number of lipid phases are indicated in each compositional domain along with schematic representations of the bilayer and lamellar structures. (Note that the excess water phase is not considered in this phase diagram.) Cholesterol molecules are represented with oval figures, a circular head group and a hydrocarbon tail.

crystal phase at temperatures between the onset and completion temperatures of transition II. It should be stressed that this region of the phase diagram is complex and we have not been able to define the phases present in the temperature zone between the completion temperature of transition I and the onset temperature of transition II. Clearly, there is progressive overlap of the two transitions as the cholesterol content increases (see Fig. 1). Above the completion temperature of transition II, all the NPGS is melted and a single cerebroside liquid crystal lamellar phase containing cholesterol exists. In contrast, at cholesterol concentrations >50 mol %, the two phase cerebroside crystal and cholesterol crystal system melts to a two phase system at ~56°C. The two phases present are a cerebroside/cholesterol (1:1 molar ratio) bilayer liquid crystal and an excess cholesterol phase.

From the structural and calorimetric data, a summary of molecular events can be proposed as follows. At temperatures below transition I, the cerebroside/cholesterol system is characterized as having solid phase immiscibility at all cholesterol concentrations. The linear decrease of apparent enthalpy for transition II as the cholesterol content increases suggests that as the temperature is increased, cholesterol removes cerebroside from the pure cerebroside lamellar domains by intermolecular association. Cholesterol intercalates into NPGS lamellae by disrupting and/or replacing NPGS-NPGS hydrogen bonds at the interface and/or head group region. As the NPGS-NPGS hydrogen bond matrix is unusually stable, the process of insertion is not favored and is energy requiring. In particular, at low temperatures the cerebroside hydrogen bond matrix is less labile, preferring NPGS-NPGS rather than NPGS-cholesterol intermolecular associations. These strong cerebroside-cerebroside intermolecular associations exclude cholesterol from the crystalline cerebroside bilayers low temperatures. At higher temperatures the NPGS-NPGS associations become more labile. This results in disruption of the cerebroside intermolecular hydrogen bonding and partial molecular disorder. Cholesterol can now insert into the bilayers, further disrupt cerebroside-cerebroside contacts, and ultimately depress the crystal → liquid crystal transition temperature to ~56°C. Below 50 mol % cholesterol, an excess unmelted phase of stable NPGS bilayers remains. Only upon heating beyond transition II to melt the cerebroside hydrocarbon chains and disrupt the hydrogen bond matrix, is the remaining cerebroside miscible in the preexisting cholesterol-containing NPGS bilayers. The two lipid component system is characterized as a homogeneously mixed cerebroside/cholesterol liquid crystal phase. At temperatures above transition II, cholesterol present in excess of 50 mol % exists as a separate phase. The low temperature solid crystalline phases are reobtained by cooling and equilibrating at $T < T_I$ (initial). Presumably NPGS-NPGS hydrogen bond associations become more favored with reduction of temperature and, as a result, stable cerebroside-cerebroside intermolecular association occurs and cholesterol is excluded. Cerebroside-cerebroside contacts presumably yield lateral aggregation, which ultimately produce a separated cerebroside phase.

The proposed molecular model is of particular interest from a molecular viewpoint because it demonstrates both similarities and differences to phosphatidylcholine-cholesterol (28, 29), and sphingomyelin-cholesterol lipid dispersions (30–32). At low temperatures, Mabrey et al. (28) demonstrated that DPPC-cholesterol dispersions exhibit the formation of a 4:1 DPPC-cholesterol molecular complex that results in solid phase immiscibility with any excess DPPC gel phase. Spin-label studies by Shimshick and McConnell (29) previously suggested two solid phases at <20 mol % cholesterol. Similarly, palmitoylsphingomyelin-cholesterol (30–31), stearoylsphingomyelin-cholesterol (32), and lignocerylsphingomyelin-cholesterol (31) dispersions are thought to exhibit two distinctly different gel phases that coexist at low temperatures; cholesterol-rich and cholesterol-poor sphingomyelin gel phases. Although NPGS-cholesterol dispersions also demonstrated solid phase immiscibility, the major difference from the behavior of phospholipid-cholesterol and sphingomyelin-cholesterol dispersions is that cholesterol is not miscible in the NPGS crystal phase and forms a separate solid phase at low temperatures. It is only at higher temperatures that cholesterol is solubilized into the cerebroside bilayers. At these temperatures an NPGS crystal phase coexists with a NPGS-cholesterol containing liquid crystal phase. Therefore, while cholesterol is readily incorporated into phospholipid bilayers at all temperatures, it is only upon heating to sufficiently high temperatures that incorporation of cholesterol into NPGS bilayers is favored. Both phosphatidylcholine and sphingomyelin dispersions containing ~50% cholesterol exhibit a very broad noncooperative transition (28, 30) (see also, Fig. 7 *a*). In contrast cerebroside-cholesterol dispersions undergo a relatively sharp, $\Delta T_{1/2}$ = ~8°C, more cooperative transition between 50–60°C (see Figs. 1 and 5). This is unique to the cerebroside-cholesterol system and may in part be explained in terms of the ability of cerebroside to associate preferentially with other cerebroside molecules as compared with phospholipids. This preferred association ensures the formation of an ordered crystal state that undergoes a crystal → liquid crystal transition, albeit at a depressed temperature, in the presence of cholesterol. The mode of association is attributed to intermolecular hydrogen bonding and has been suggested to be mediated via the galactose, sphingosine hydroxyl, and amide moieties of the glycosphingolipid (9).

Under the thermal regimen used in this study (see Methods), transition I at 50–60°C always occurs in the presence of 50 mol % cholesterol. In a recent calorimetric study, Linington and Rumsby (19) demonstrated that increasing cholesterol contents diminish the enthalpy of the gel-liquid crystal transition of bovine brain cerebrosides.

Interestingly, the peak temperature of this gel → liquid crystal transition for cerebroside-cholesterol mixtures appears to occur at approximately the same temperature range as that of pure bovine brain cerebrosides without cholesterol. The enthalpy data indicate that ~34 mol % cholesterol eliminates the gel → liquid crystal transition. Much less cholesterol is necessary to eliminate the mixed bovine brain cerebroside gel → liquid crystal transition than in our study (i.e., ~50 mol % cholesterol to remove transition II). This apparent discrepancy may be rationalized in terms of the amide-linked 2-hydroxy fatty acid containing cerebroside (HFA-Cer) fraction of the mixed bovine brain cerebrosides used in reference 19. The HFA-Cer fraction has been suggested to disrupt and prevent formation of the unusually stable gel state observed for *N*-acylcerebrosides (10). Such an effect on the pure cerebroside gel state, in addition to the mixed fatty acid content of natural cerebrosides, may alter the solubility of cholesterol in bovine brain cerebrosides and reduce the amount of cholesterol necessary to fluidize the cerebroside gel state completely. Although no thermal transition is readily observed at 40 mol % cholesterol in reference 19, the exact thermal regimen is not reported and may differ from ours. Nevertheless, it can be concluded from our results that the effect of cholesterol upon the cerebroside crystal phase is such that, even though both components exhibit solid phase immiscibility at low temperature, the temperature at which NPGS bilayers melt is reduced considerably (~30°C) in the presence of cholesterol (see Figs. 1 and 5).

NPGS-Cholesterol-Dipalmitoylphosphatidylcholine Bilayers

For the ternary lipid system, the calorimetric thermograms shown in Fig. 7 demonstrate no detectable thermal transitions over the 0 to 23.1 mol % cerebroside concentration range. In contrast, at greater concentrations an endothermic transition progressively dominates the thermal behavior of the DPPC/cholesterol/NPGS dispersions. Structural studies show no gross structural changes over the 22 to 90°C temperature range for dispersions containing <20 mol % cerebroside other than a reduction in lamellar periodicity and slight increase in chain packing disorder. At >20 mol % NPGS, a second lamellar phase is observed due to the presence of excess NPGS bilayers (Figs. 9 and 10). Based on calorimetric and x-ray diffraction studies, the transition enthalpy at >20 mol % NPGS is associated with the melting of the excess NPGS crystal bilayer to the liquid crystal bilayer. Extrapolation of the enthalpy of the broad endotherm at low cerebroside concentrations to the pure hydrated NPGS crystal → liquid crystal enthalpy (17.5 kcal/mol NPGS) is consistent with the observed structural changes and the assignment of the transition as a cerebroside crystal → liquid crystal transition.

At 22°C the incorporation of up to ~20 mol % of cerebroside into the DPPC/cholesterol bilayers results in a single lamellar periodicity that decreases slightly in a linear fashion (Fig. 10). This suggests that the three lipid components are miscible at these concentrations. Above the cerebroside saturation concentration, the lamellar periodicity no longer changes and cerebroside in excess of ~23 mol % forms a separate cerebroside phase. The saturation concentration for cerebroside as determined by x-ray diffraction, ~23 mol %, corresponds well with the limit derived by extrapolation of the calorimetric data, 22 ± 3 mol % NPGS.

The temperature-composition phase diagram, derived from the calorimetric and x-ray diffraction data, is presented in Fig. 14. The composition range of the three components studied represents a single section of the ternary lipid phase diagram of cholesterol, phosphatidylcholine, and cerebroside corresponding to an equimolar cholesterol/phosphatidylcholine ratio (see Fig. 14, inset). Phase separation of cerebroside is obtained at concentrations >23 mol % NPGS where a DPPC/cholesterol (1:1) bilayer phase containing 22 ± 3 mol % cerebroside coexists with an excess cerebroside phase. The excess NPGS crystal phase progressively melts into the DPPC/cholesterol-rich liquid crystal until at $T > 82$°C (T_m of NPGS) a single lamellar liquid crystal phase of DPPC/cholesterol/cerebroside exists.

Calorimetric studies by Ladbrooke et al. (33) and more recently by Linington and Rumsby (19) demonstrate that hydrated myelin total lipid extract (including cholesterol) exhibited no thermal liquid transitions over the 0–100°C temperature range. However, the removal of the cholesterol fraction resulted in the expression of complex endothermic transitions associated with the phospholipid-galactocerebroside fractions. It was interpreted that cholesterol exerts the well-recognized fluidization effect upon the polar lipid fraction. Our calorimetric and x-ray diffraction results on mixtures containing equimolar concentrations of cholesterol/phospholipid and ~20 mol % cerebroside are consistent with these earlier data from naturally occurring lipid dispersions (see Figs. 7 and 10).

Equimolar proportions of cholesterol and phospholipid were chosen in this study since these proportions occur in myelin membrane. The proportions of cholesterol/phospholipid/cerebroside found in myelin are depicted in Fig. 14 (see vertical dashed line). Our model studies suggest that although myelin has a relatively high content of cerebroside, its composition falls at a concentration such that all cerebroside is miscible in the membrane bilayer phase. Note that glycosphingolipids in general tend to be asymmetrically disposed in biomembranes (34, 35). Recent studies have shown that cerebroside is preferentially, if not totally, located on the external (extracellular) monolayer of myelin membrane (36, 37). Such a concentration of galatocerebroside would result in ~40 mol % cerebroside in the extracellular monolayer. If protein-lipid interactions are neglected for this predominantly lipid containing membrane, such a situation, according to our

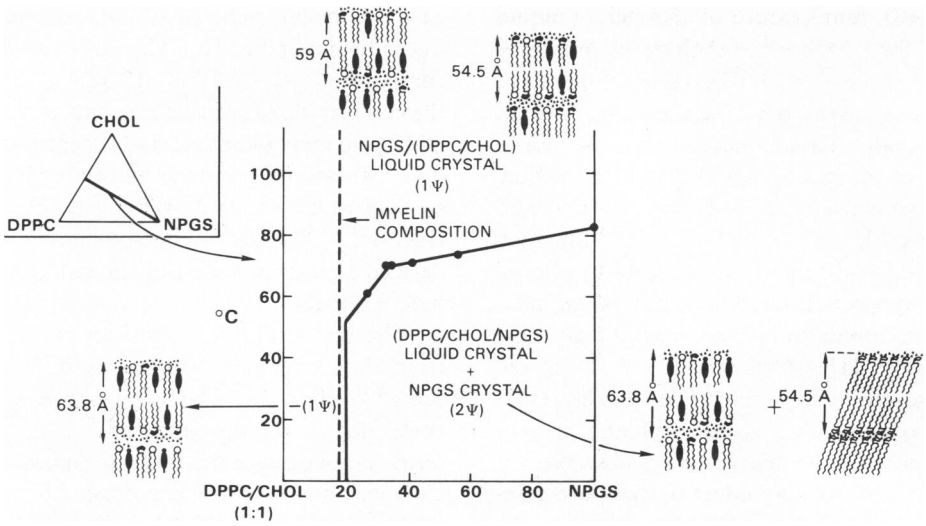

FIGURE 14 DPPC/cholesterol (1:1 molar ratio)/NPGS section of the temperature-composition phase diagram of ternary (DPPC/cholesterol/NPGS) lipid system at 70% H_2O by weight. Temperature of the NPGS crystal → liquid crystal transition (filled circles) are indicated. (*Inset* represents section of ternary lipid-phase diagram studied.) The number of lipid phases are indicated in each compositional domain along with schematic representations of the bilayer structures. (Note that the excess water phase is not considered in this phase diagram.) Phospholipid molecules are represented with closed circle head groups, cerebroside molecules are represented with closed circle head groups. The composition of myelin membranes is indicated by the vertical dashed line.

model studies using DPPC/cholesterol at a 1:1 molar ratio, would result in phase separation of the galactocerebroside (see Fig. 14). Interestingly, however, Caspar and Kirschner (38) have suggested that cholesterol is asymmetrically disposed such that a molar ratio of 1:1 (cholesterol/polar lipid) occurs in the outer extracytoplasmic monolayer. Such a cholesterol/polar lipid ratio should provide sufficient sterol to maintain the cerebroside-rich extracytoplasmic monolayer in a fluidlike liquid crystal state.

Although the exact role of cerebroside is unclear, the unusually high content in myelin strongly suggests a structural role. The hydrogen bonding capability of cerebroside may be of considerable importance to the insulating property of the myelin sheath. Hydrogen bonding would allow not only an increased intermolecular association between lipid molecules at the membrane surface, it may also serve to structure water into a more immobile water layer near the membrane surface. Alternatively, water may be excluded from the immediate lipid head group-hydrocarbon interface due to preferential head group associations. In addition to the potential capability of cerebrosides to structure and/or exclude water from the membrane interface, cholesterol has been shown to reduce effectively penetration of water into phospholipid bilayers (39). Together, cerebroside and cholesterol, which constitute ~60 mol % of the lipid in myelin (or >80 mol % in the outer monolayer for the case of an asymmetric arrangement as discussed above), may be expected to increase impermeability, reduce water activity at the membrane surface, and reduce the ability of water and ions to move or to be transported across the myelin sheath (i.e., increase electrical resistance). Of particular relevance to these points is that in the dysmyelinating (leukodystrophic) disorder, Pelizaeus-Merzbacher's disease, in which there is aberrant nerve impulse conduction in peripheral nervous system neurons, cerebroside content is markedly reduced in the myelin sheath (40).

We thank Drs. E. Oldfield and R. Skarjune for supplying NPGS. We thank Drs. D. Atkinson and D. M. Small for useful discussions and David Jackson for technical assistance. We thank Irene Miller for assistance in the preparation of this manuscript.

This work was supported by National Institutes of Health Research grant HL-26335 and Training grants HL-07291 and HL-07429.

Received for publication 8 November 1983 and in final form 13 June 1984.

REFERENCES

1. Norton, W. T. 1981. Biochemistry of myelin. *In* Demyelinating Disease: Basic and Clinical Electrophysiology. S. G. Waxman and J. M. Ritchie, editors. Raven Press, New York. 93–121.
2. Reiss-Husson, F. 1967. Structure des phases liquide-cristallines de differents phospholipides, monoglycerides, sphingolipides, anhydres ou en presence d'eau. *J. Mol. Biol.* 25:363–382.
3. Abrahamsson, S., I. Pascher, K. Larsson, and K. -A. Karlsson. 1972. Molecular arrangements in glycosphingolipids. *Chem. Phys. Lipids.* 8:152–179.
4. Pascher, I., and S. Sundell. 1977. Molecular arrangements in sphingolipids. The crystal structure of cerebroside. *Chem. Phys. Lipids.* 20:175–191.
5. Fernandez-Bermudez, S., J. Loboda-Cackovic, H. Cackovic, and R. Hosemann. 1977. Structure of cerebrosides. I. Phrenosine at 23°C and 66°C. *Z. Naturforsch. Teil. C. Biochem. Biophys. Biol. Virol.* 32:362–364.
6. Hosemann, R., J. Loboda-Cackovic, H. Cackovic, S. Fernandez-

Bermudez, and F. J. Balta-Calleja. 1979. Structure of cerebrosides. II. Small angle x-ray diffraction study of cerasine. *Z. Naturforsch. Teil. C. Biochem. Biophys. Biol. Virol.* 34:1121–1124.

7. Bunow, M. R. 1979. Two gel states of cerebrosides: calorimetric and Raman spectroscopic evidence. *Biochim. Biophys. Acta.* 574:542–546.
8. Freire, E., D. Bach, M. Correa-Freire, I. Miller, and Y. Barenholz. 1980. Calorimetric investigation of the complex phase behavior of glucocerebroside dispersions. *Biochemistry.* 19:3662–3665.
9. Ruocco, M. J., D. Atkinson, D. M. Small, R. P. Skarjune, E. Oldfield, and G. G. Shipley. 1981. X-ray diffraction and calorimetric study of anhydrous and hydrated *N*-palmitoylgalactosylsphingosine (cerebroside). *Biochemistry.* 20:5957–5966.
10. Curatolo, W. 1982. Thermal behavior of fractionated and unfractionated bovine brain cerebrosides. *Biochemistry.* 21:1761–1764.
11. Bach, D., B. Sela, and I. R. Miller. 1982. Compositional aspects of lipid hydration. *Chem. Phys. Lipids.* 31:381–394.
12. Ruocco, M. J. A. 1983. Molecular interaction of cerebroside with phospholipid and cholesterol. Ph.D. dissertation. Boston University, Boston, MA 1–338.
13. Ruocco, M. J., and G. G. Shipley. 1983. Hydration of *N*-palmitoylgalactosylsphingosine compared to monosaccharide hydration. *Biochim. Biophys. Acta.* 735:305–308.
14. Neuringer, L. J., B. Sears, and F. B. Jungalwala. 1979. Deuterium NMR-studies of phospholipid-cerebroside bilayers. *Biochim. Biophys. Acta.* 558:325–329.
15. Skarjune, R., and E. Oldfield. 1979. Physical studies of cell surface and cell membrane structure. Deuterium nuclear magnetic resonance investigation of deuterium-labelled *N*-hexadecanoylgalactosylceramides (cerebrosides). *Biochim. Biophys. Acta.* 556:208–218.
16. Skarjune, R., and E. Oldfield. 1982. Physical studies of cell surface and cell membrane structure. Deuterium nuclear magnetic resonance studies of *N*-palmitoylglucosylceramide (cerebroside) head group structure. *Biochemistry.* 21:3154–3160.
17. Clowes, A. W., R. J. Cherry, and D. Chapman. 1971. Physical properties of lecithin-cerebroside bilayers. *Biochim. Biophys. Acta.* 249:301–317.
18. Correa-Freire, M. C., E. Freire, Y. Barenholz, R. L. Biltonen, and T. E. Thompson. 1979. Thermotropic behavior of monoglucocerebroside-dipalmitoylphosphatidylcholine multilamellar liposomes. *Biochemistry.* 18:442–445.
19. Linington, C., and M. G. Rumsby. 1981. Galactosyl ceramides of the myelin sheath: thermal studies. *Neurochem. Int.* 3:211–218.
20. Bunow, M. R., and I. W. Levin. 1980. Molecular conformations of cerebrosides in bilayers determined by Raman spectroscopy. *Biophys. J.* 32:1007–1022.
21. Ruocco, M. J., G. G. Shipley, and E. Oldfield. 1983. Galactocerebroside-phospholipid interactions in bilayer membranes. *Biophys. J.* 43:91–101.
22. Ladbrooke, B. D., R. M. Williams, and D. Chapman. 1968. Studies on lecithin-cholesterol-water interactions by differential scanning calorimetry and x-ray diffraction. *Biochim. Biophys. Acta.* 150:333–340.
23. Ladbrooke, B. D., and D. Chapman. 1969. Thermal analysis of lipids, proteins, and biological membranes. A review and summary of some recent studies. *Chem. Phys. Lipids.* 3:304–356.
24. Lecuyer, H., and D. G. Dervichian. 1969. Structure of aqueous mixtures of lecithin and cholesterol. *J. Mol. Biol.* 45:39–57.
25. Lee, A. G. 1977. Lipid phase transitions and phase diagrams. II. Mixtures involving lipids. *Biochim. Biophys. Acta.* 472:285–344.
26. Presti, F. T., R. J. Pace, and S. I. Chan. 1982. Cholesterol-phospholipid interaction in membranes. 2. Stoichiometry and molecular packing of cholesterol-rich domains. *Biochemistry.* 21:3831–3835.
27. Loomis, C. R., G. G. Shipley, and D. M. Small. 1979. The phase behavior of hydrated cholesterol. *J. Lipid Research.* 20:525–535.
28. Mabrey, S., P. L. Mateo, and J. M. Sturtevant. 1978. High-sensitivity scanning calorimetric study of mixtures of cholesterol with dimyristoyl- and dipalmitoylphosphatidylcholines. *Biochemistry.* 17:2464–2468.
29. Shimshick, E. J., and H. M. McConnell. 1973. Lateral phase separations in binary mixtures of cholesterol and phospholipids. *Biochem. Biophys. Res. Commun.* 53:446–451.
30. Calhoun, W. I., and G. G. Shipley. 1979. Sphingomyelin-lecithin bilayers and their interaction with cholesterol. *Biochemistry.* 18:1717–1722.
31. Estep, T. N., D. B. Mountcastle, Y. Barenholz, R. L. Biltonen, and T. E. Thompson. 1979. Thermal behavior of synthetic sphingomyelin-cholesterol dispersions. *Biochemistry.* 18:2112–2117.
32. Estep, T. N., E. Freire, F. Anthony, Y. Barenholz, R. L. Biltonen, and T. E. Thompson. 1981. Thermal behavior of stearoylsphingomyelin-cholesterol dispersions. *Biochemistry.* 20:7115–7118.
33. Ladbrooke, B. D., T. J. Jenkinson, V. B. Kamat, and D. Chapman. 1968. Physical studies of myelin. I. Thermal analysis. *Biochim. Biophys. Acta.* 164:101–109.
34. Steck, T. L., and G. Dawson. 1974. Topological distribution of complex carbohydrates in the erythrocyte membrane. *J. Biol. Chem.* 249:2135–2142.
35. Stoffel, W., and W. Sorgo. 1976. Asymmetry of lipid-bilayer of Sindbis virus. *Chem. Phys. Lipids.* 17:324–335.
36. Linington, C., and M. G. Rumsby. 1978. On the accessibility and localisation of cerebrosides in central nervous system myelin. *Adv. Exp. Med. Biol.* 100:263–273.
37. Linington, C., and M. G. Rumsby. 1980. Accessibility of galactosylceramides to probe reagents in central nervous system myelin. *J. Neurochem.* 35:983–992.
38. Caspar, D. L. D., and D. A. Kirschner. 1971. Myelin membrane structure at 10 Å resolution. *Nature New Biology.* 231:46–52.
39. Simon, S. A., T. J. McIntosh, and R. Latorre. 1982. Influence of cholesterol on water penetration into bilayers. *Science (Wash. DC).* 216:65–67.
40. Witter, B., H. Debuch, and H. Klein. 1980. Lipid investigation of central and peripheral nervous system in connatal Pelizaeus-Merzbacher's disease. *J. Neurochem.* 34:957–962.